

## Development and *in vitro* evaluation of tamoxifen and doxycycline loaded lipid-polymer hybrid nanoparticles for anticancer therapy

Qurat ul Ain<sup>1</sup>, Muhammad Adil Rasheed<sup>1\*</sup>, Imran Tariq<sup>2</sup>, Muhammad Ovais Omer<sup>1</sup>, Muhammad Yasir Zahoor<sup>3</sup>

<sup>1</sup>Department of Pharmacology and Toxicology, Faculty of Biosciences, University of Veterinary and Animal Sciences, Lahore, Pakistan

<sup>2</sup>Punjab University College of Pharmacy, University of the Punjab, Lahore, 54000, Pakistan

<sup>3</sup>Institute of Biochemistry and Biotechnology, Faculty of Biosciences, University of Veterinary and Animal Sciences, Lahore, Pakistan

\*Corresponding author's email: dr\_aadil@uvas.edu.pk

Received: 06 December 2024 / Accepted: 11 March 2025 / Published Online: 25 March 2025

### Abstract

Lipid-polymer hybrid nanoparticles (LPHNPs) are innovative composite structures featuring a core-shell design, with a polymeric nanoparticle core surrounded by PEGylated lipid layers. This architecture combines liposome circulation with nanoparticle strength, offering a promising solution for multidrug-resistant cancers. The current study aimed to develop an integrated platform that leverages these advantageous characteristics. To achieve this, Tamoxifen-loaded nanoparticles were formulated using emulsion solvent evaporation technique with PLGA poly (lactic-co-glycolic) acid polymer, while Doxycycline-containing liposomes were developed through a film hydration method. These two components were then combined to fabricate LPHNPs. A range of physicochemical and structural analyses, including dynamic light scattering (DLS), laser diffraction analysis (LDA), and scanning electron microscopy (SEM), were performed. Cellular cytotoxicity was quantitatively assessed using the MTT assay, and biocompatibility was evaluated through *in vivo* acute toxicity tests on female albino mice. The average hydrodynamic sizes of Tamoxifen and Doxycycline formulations were  $198.80 \pm 2.10$  nm and  $100.5 \pm 1.29$  nm, respectively. After coating Tamoxifen nanoparticles with Doxycycline liposomes, resultant LPHNPs exhibited a diameter of  $200.4 \pm 2.51$  nm and a zeta potential of  $4.45 \pm 2.51$  mV. Notably, LPHNPs demonstrated a significant increase in cytotoxicity ( $p < 0.001$ ) and showed reduced *in vivo* toxicity compared to free drugs, with no discernible toxicity observed in histopathology of vital organs, confirming their safety and efficacy.

**Keywords:** Cytotoxicity, Tamoxifen, Doxycycline, Nanoparticles, Cancer

### How to cite this article:

Qurat ul Ain, Rasheed MA, Tariq I, Omer MO and Zahoor MY. Development and *in vitro* evaluation of tamoxifen and doxycycline loaded lipid-polymer hybrid nanoparticles for anticancer therapy. Asian J. Agric. Biol. 2025: 2024256. DOI: https://doi.org/10.35495/ajab.2024.256

This is an Open Access article distributed under the terms of the Creative Commons Attribution 4.0 License. (<https://creativecommons.org/licenses/by/4.0>), which permits unrestricted use, distribution, and reproduction in any medium, provided the original work is properly cited.

## **Introduction**

Combination therapy in cancer treatment has proven to be more effective than single-drug approaches. This approach can notably decrease side effects, enhance efficacy, and possibly address multidrug resistance, a major obstacle to anticancer chemotherapy's effectiveness (Ali et al., 2021a). Combination chemotherapy harnesses synergistic effects from various drugs to enhance therapeutic outcomes and potentially mitigate side effects by triggering cell apoptosis through diverse signaling pathways (Liu et al., 2021; Saif et al., 2024b). To achieve optimal enhancement, it is imperative to co-localize therapeutic agents with distinct mechanisms of action within tumor cells. Using these nano drug delivery techniques, Anticancer medications can exhibit enhanced solubility and bioavailability, increased potency even at lower effective dosages, decreasing the tumor's volume or viability of cancer cells in comparison to when therapies were given separately (Saif et al., 2024a).

Breast cancer is the primary cause of cancer related deaths among women worldwide. Estrogen receptor-positive tumors are present in about 75% of cases of breast cancer, for which Tamoxifen serves as the primary treatment approach (Ismail et al., 2022). Tamoxifen, an antiestrogen, is effectively employed in clinical breast cancer treatment for both pre- and post-menopausal women. However, when Tamoxifen is taken orally, side effects include pulmonary embolism, hot flashes, visual abnormalities and deep vein thrombosis and some types of cancer may occur. Encapsulating Tamoxifen into a nanoparticulate system offers the potential to modify its pharmacokinetic parameters, thereby reducing side effects and enhancing system efficacy. PLGA nanocarriers have been explored to transport drugs to their intended target sites. Due to their biocompatibility and biodegradability, PLGA nanoparticles present compelling options for the systemic delivery of Tamoxifen. Doxycycline is FDA approved antibiotic and has a wide range of antimicrobial activities and a well-defined safety profile. It was originally used to treat respiratory ailments. In addition, Doxycycline has an excellent safety history when used for a prolong time and is a well-tolerated drug. Pregnant women and children can also use doxycycline safely because it has no record of teratogenic effects, and has anti-proliferative and cytotoxic effects (Chhipa et al., 2005; Markowska et

al., 2019). Studies showed its effectiveness against various types of cancers i.e., breast, colon, mesothelioma, osteosarcoma, renal, prostate, and melanoma cell lines (Fife and Sledge Jr, 1995; Onoda et al., 2006; Rubins et al., 2001; Seftor et al., 1998). Protein formation is inhibited by Doxycycline in the way to disrupt the binding of activated aminoacyl transfer RNAs with 30S bacterial ribosomal subunit. The 28S mitochondrial ribosome of mammalian cells is like a 30S bacterial ribosomal unit, therefore, the mitochondrial biogenesis in mammalian cell is inhibited with the use of Doxycycline. It also inhibits self-renewal of Breast cancer stem cells and its proliferation because it prevents the regeneration of those factors that develop stem cells, e.g., Sox2-SRY (Sex Determining Region Y)-box 2, Oct4 (Octamer-binding transcription factor) 4, c-myc (Cellular Myelocytomatosis Viral Oncogene Homolog) and Nanog (Nanog Homeobox). These factors play important roles in maintaining stem cell properties and are involved in the self-renewal and pluripotency of stem cells. Doxycycline causes downregulation of EMT (Epithelial to mesenchymal transition) related markers as a result it causes EMT inhibition, BCSCs migration and invasion (Markowska et al., 2019; Zeng et al., 2020). Doxycycline primarily inhibits MMP-2 and MMP-9, making it a well-tolerated and more efficient matrix metalloproteinase inhibitors within the tetracycline class of drugs (Onoda et al., 2004). Studies indicated that doxycycline exhibits anti-angiogenic effects (Gu et al., 2001).

Drug encapsulation within liposomal or lipid-based delivery systems improves pharmacokinetic and pharmacodynamic properties and enhances drug efficacy, that is a key focus of research in drug delivery and design. Liposomes have been shown to boost the therapeutic index of various drugs by either increasing potency or reducing toxicity. By encapsulating drugs in liposomes, their distribution can be modified, restricting access to intact cells while facilitating entry into malignant cells (Karami, 2023). The Primary objective of current study was to formulate innovative lipid polymer hybrid nanoparticles (LPHNPs), consisting of a liposomal membrane surrounding a core of nanoparticles. The current study offered a synergistic approach using this nanocarrier system for cancer cell therapy by releasing two different drug moieties. Formulations containing Tamoxifen and Doxycycline were evaluated for their diameter distribution and surface charge using DLS and LDA, respectively. Morphological features were

analyzed using Scanning Electron Microscopy (SEM). Furthermore, *in vitro* cell viability assays were performed on both breast cancer cells and Vero cells. IC<sub>50</sub> concentration was calculated for free Tamoxifen, Tamoxifen-loaded PLGA nanoparticles, free Doxycycline, Doxycycline-loaded liposomes, and lipid polymer hybrid nanoparticles (LPHNPs). Acute *in vivo* toxicity studies were carried out on female albino mice, encompassing blood biochemistry studies and histological investigations (Ali et al., 2023).

## Material and Methods

Tamoxifen citrate was purchased from Wuhan's Pharmaceutical, Doxycycline Hyclate was obtained as gift sample from Rasco pharmaceutical (Lahore, Pakistan). DPPC (Dipalmitoylphosphatidylcholine), DPPE-mPEG5000, DPPG, PLGA (Resomer® RG 503 H, PVA, Mowiol 4–88, Polysorbate 80 (Tween 80), MTT dye were acquired from Sigma Aldrich Chemical co. (St. Louis, MO). Organic solvents of HPLC quality, chloroform, methanol, ethanol, ethyl acetate were acquired from the postgraduate laboratory of The College of Pharmacy, Punjab University. Sterile filtered ultrapure miliQ and RO water obtained from WTO laboratory UVAS (Lahore, Pakistan), chitosan, acetic acid (1% v/v), dialysis membrane, NaOH, HCL, penicillin, streptomycin, amphotericin B, FBS, trypsin-EDTA (0.25%), bicarbonate buffer, syringe filter (0.22µm), DMSO (10%), DMEM and RPMI 1640 medium, all materials were analytical grade, obtained from same source and used as received. PBS was freshly prepared, sterilized through filtration, and stored in the refrigerator for subsequent use.

### Development of Tamoxifen loaded nano carriers

The emulsion solvent evaporation technique was used to prepare PLGA nanoparticles loaded with tamoxifen and blank nanoparticles. In short, 1 mg/mL of tamoxifen was solubilized in ethyl acetate to create a tamoxifen stock solution. A 100 milligram PLGA polymer was mixed in 5 milliliters of ethyl acetate consisting of 2 milligrams of tamoxifen. To create nanoparticles, the organic phase was subjected to filtration with syringe filter (0.2 µm), then added dropwise to an aqueous medium of PVA solution (1% w/v). After forming an o/w emulsion, it was uniformed for 10 minutes at 15,000 rpm using an Ultra-Turrax

homogenizer. 1 mL (0.10%) of chitosan was introduced to the created nano-emulsion. The ultrapure water was added dropwise to make up the volume up to 30 mL, and left it overnight for evaporation to enhance nanoprecipitation. Blank nanoparticles were prepared using a similar process, with the exception of adding the Tamoxifen stock solution. The next day, the entire organic solvent was evaporated, and nanoparticle suspension was spun using a centrifuge for 45 seconds at 2000x to remove any flakes or agglomerates. In order to remove the drug that was not encapsulated from the nanoparticles, formed pellet was disposed of and supernatant was cleaned with water. Nanoparticles were washed twice for 20 min at 16000x g. After that, suspension of nanoparticles was freeze-dried using a lyophilizer with a cryoprotectant such as PVA (0.2% w/v). Until further examination, lyophilized nanoparticles were kept between 2 and 8 °C (Duse et al., 2019).

### Development of Doxycycline liposomal carriers

DPPC, DPPG, and DPPE-mPEG5000 (85:10:5) were dissolved in methanol and chloroform solution. Doxycycline added in these lipids at a ratio of 1:20 for drug-loaded liposomes. At 45 °C, a rotary evaporator was used to evaporate organic solvents. To create the liposomes, 1 mL of PBS (pH 7.4) was used for film hydration process, which was then vigorously shaken. To convert the pre-formed liposomes from multilamellar liposomes to unilamellar liposomes, sonicated for 40 minutes in a bath-style sonicator. (Mahmoud et al., 2018).

### Formation of lipid polymer hybrid nanoparticles

The fusion process was used to create lipid layer on particle surface. In brief, a suitable amount of DOXY LPs was mixed to TMX NPs suspension and blended properly. Formulation was subsequently sonicated for 40 min, and incubated for an hour, a self-organized lipid bilayer spontaneously fused to surface of nanoparticles (Schäfer et al., 2008; Vickers, 2017; Rasool et al., 2024).

### Hydrodynamic diameter and ζ potential assessment

Dynamic light scattering and laser doppler anemometry were used, outfitted with a 10 mW HeNe laser operating at 633 nm and a scattered light

detection system positioned at 173° at 25°C. The machine automatically adjusted laser attenuation and measurement positions for each measurement. Particle size, PDI, and charge on surface were consistently observed for all samples using a disposable capillary cell. Before analysis, samples were diluted (1:100) with pure water. When interpreting results, water viscosity (0.88 mPa.s) and refractive index (1.33) were taken into consideration. Results are presented as mean ± S.D.

### Efficiency of drug encapsulation (EE%)

The ratio of the amount of encapsulated substance in the liposome to the total weighted substance is known as the encapsulation efficiency (Zhang et al., 2004). Column chromatographic separation approach is helpful for separating free drugs from drug-loaded liposomes, known as gel filtration method since Sephadex and Sepharose columns are the most widely used chromatographic columns. Typically, separation takes place in a column filled with porous beads like Sephadex and agarose gel. Larger particles, such as liposomes, cannot enter the pores during the elution process and can be eluted more quickly than comparatively low molecular weight particles, which can enter the pores more readily and stay in them for extended time period. This allows the separation of drug-encapsulated liposomes from non-encapsulated drug by utilizing the differential in retention time (Lin and Qi, 2021). The Sephadex G-50 column is first filled with 0.5 mL of liposomal suspension. Phosphate Buffer Solution (pH 7.4) is then added as the eluent for liposome purification, flowing at a rate of 0.5 mL/min. One tube is used to collect each 2 mL of eluate. The eluate's turbidity is monitored, or the drug and lipid concentrations in the eluate are measured, in order to collect the liposomes (Yang et al., 2013). Initially, the liposomes were eluted with PBS (pH 6.5) after being separated from the free drug by gel filtering through a SephadexG-50 column (AlMajed et al., 2022; Lin and Qi, 2021; Yang et al., 2013).

The solvent extraction method revealed EE % of PLGA nanoparticles loaded with Tamoxifen. Untrapped medication was separated from 1 mL of freshly generated nanoparticle suspension by centrifuging it at 16000x g for 20 minutes using centrifuge. After supernatant was removed, acetonitrile was poured in an equivalent volume. In a similar manner, 1 mL of acetonitrile was added to nanoparticle pellet to dissolve it, drug was fully extracted by sonicating mixture for 15 minutes.

Absorbance measured using a UV/VIS spectrophotometer at 230 nm (Pandey et al., 2015; Yu et al., 2020). Without drugs nanoparticles were used as a blank control. Using calibration curves created in same media with known doses of tamoxifen, amount of medication encapsulated was measured.

The standard curve for Doxycycline was formed in both ethanol and PBS 7.4 phosphate buffer solution. The EE (%) was calculated using equation 1, and determine the loading capacity using equation 2.

$$EE(\%) = \frac{\text{Amount of drug encapsulated}}{\text{Total Drug}} \times 100 \quad \text{-----}$$

Equation 1

$$LC(\%) = \frac{\text{Amount of drug encapsulated}}{\text{Dry weight of nanoparticles}} \times 100 \quad \text{-----}$$

Equation 2

### Structure analysis by scanning electron microscopy (SEM)

It is a widely employed technique for characterizing nanomaterials and nanostructures. Signals resulting from electron-sample interactions provide insights into the sample's surface morphology (texture) and chemical composition (Sharmin and Bhuiyan, 2019). Subsequently, sterilized nanoparticles were securely mounted on SEM stubs using adhesive tape. NPs were then placed in SEM sample chamber and scanned at various magnifications ranging from ×15,000 to ×35,000 and an operating voltage of 20–30 kV (Verma and Maheshwari, 2018).

### In vitro drug release analysis

Release pattern of TMX NPs was tested in PBS (pH 7.4) with 1% (v/v) tween 80. The drug-containing nanoparticle pellet (0.5 mg) was reconstituted in 5 mL of PBS (pH 7.4) containing tween 80 (1 %), incubated at 100 rpm at 37 °C in a shaking incubator. A 0.5 mL sample was taken every day for next few days at predetermined times. Material was separated from supernatant after it was centrifuged for 10 minutes at 15000x g. The pellet was again suspended in 1% tween 80 in fresh PBS (pH 7.4) and added back to initially formed nanoparticle suspension to ensure sink conditions. Tamoxifen content in supernatant was found using spectrophotometer at 236 nm wavelength. Following experiment, acetonitrile was used to dissolve pellet of nanoparticle to determine remaining drug content within nanoparticles (Ahmad et al., 2020; Pérez et al., 2012).

### Cell culture protocols

The *in vitro* cytotoxic potential was assessed using MTT assay. MCF-7 cells and Vero cells were obtained from the Quality Operation Laboratory at UVAS. These cells were cultured in a 96-well plate and maintained at 37 °C with 7 % CO<sub>2</sub> under humidified conditions. Culture medium was refreshed every other day, cells were grown as single layer (Senthilraja and Kathiresan, 2015). Formulation samples were serially diluted in DMEM at a conc. of 12.6 g/L. These included various concentrations of free Tamoxifen, Tamoxifen-loaded NPs (200-0.78 µg/mL), free Doxycycline, Doxycycline-loaded LPs (200-0.78 µg/mL), and LPHNPs (200-0.78 µg/mL). The depleted growth medium from 96-well plates was replaced with 100 µL of each drug dilution. The cells were then incubated for 24 hours. On the following day, 100 µL of 0.25% MTT dye was added to each well and incubated for an additional 4 hours. After incubation, the MTT dye was removed, and to solubilize formazan crystals 100 µL of 10% DMSO was added. All drug formulations and combinations were tested in triplicate. Optical density of each well was measured at 570 nm using an ELISA reader (Nankali et al., 2020).

The (%) of cell growth inhibition was calculated using equation 3:

$$\text{Growth inhibition (\%)} = \left\{ 1 - \frac{\text{OD}(\text{test}) - \text{OD}(\text{blank})}{\text{OD}(\text{+ve control}) - \text{OD}(\text{blank})} \right\} \times 100 \quad \text{-----}$$

#### Equation 3

where OD<sub>test</sub>, OD<sub>+ve control</sub> and OD<sub>blank</sub> denote the average optical densities measured at 570 nm for test sample, +ve control, and blank, respectively (Abdmouleh et al., 2020).

### IC<sub>50</sub> and selectivity index (SI).

The IC<sub>50</sub> values, representing the drug concentrations required to inhibit cell growth by 50% in inoculated wells, were determined. These values were utilized to calculate the selectivity index (SI), assessing the cytotoxic specificity towards cancer cells compared to normal cells.

$$\text{Cell viability (\%)} = \left( \frac{\text{Ab}(\text{sample}) - \text{Ab}(\text{blank})}{\text{Ab}(\text{control}) - \text{Ab}(\text{blank})} \right) \times 100 \quad \text{--}$$

----- Equation 4

Here, Ab Sample and Ab Control represent optical densities of treated and untreated samples, respectively. Ab Blank refers to optical density of well containing medium without any cells. Values are presented as mean ± standard deviation (SD), with each experiment conducted in triplicate (Moin et al., 2021).

$$[\text{SI}] = \frac{\text{IC}_{50} \text{ of drug in normal cell line}}{\text{IC}_{50} \text{ of drug in cancerous cell line}} \quad \text{-----}$$

#### Equation 5

SI value below 2 suggests general cytotoxicity against normal cells, whereas values above 2 and 3 indicate good and excellent selectivity against cancerous cells, respectively (Lafi et al., 2021).

### *In vitro* cytotoxicity analysis

Different quantities of Doxycycline-loaded liposomes, properly diluted with the medium, varying from 200 µM to 0.05 µM, were employed for *in vitro* cytotoxicity. Cells lacking any liposomal formulation were regarded as a -ve control, whereas free doxycycline dissolved in DMSO was used as a normal reference. The optimal size for additional investigations was determined to be TMX NPs with mean hydrodynamic size of 198 nm, based on outcomes of cell viability assay and the physicochemical characterizations. As a result, DPPC/cholesterol/mPEG5000-DPPE liposomes loaded with Doxycycline were coated on these nanoparticles. The LPHNPs that were used to transport tamoxifen and doxycycline to the MCF-7 malignant cells were also subjected to a cell survival assessment. To achieve this, comparable amounts of all respective formulations were incubated for four hours with MCF-7 cells. After incubation, a fresh medium was used. MTT test was used next day to assess cell viability.

### *In vivo* acute toxicity evaluation

The *in vivo* acute toxicity studies were conducted on mice over a 14-day period, following guidelines set by the Organization for Economic Cooperation and Development (OECD) 425. All experiment procedures were conducted in accordance with protocols authorized by Institutional Bioethics Committee of the University of Veterinary and Animal Sciences, Lahore. Briefly, healthy female albino mice, weighing 30–35 g and aged 8–10 weeks, were procured and randomly allocated into six groups, each

consisting of three animals. All animals had unrestricted access to water and commercial laboratory chow, housed under controlled conditions with a temperature of  $22 \pm 2$  °C, relative humidity of  $60 \pm 10\%$ , and a 12-hour light/dark cycle. Group 1 received normal saline and served as the control group. Group 2 was administered free TMX, dissolved in 0.10% DMSO, while Group 3 received TMX-loaded NPs, with the Tamoxifen dose equivalent to 5 mg/kg body weight in both cases. Group 4 received free DOXY, dissolved in 0.1% DMSO, while Group 5 was treated with DOXY-loaded LPs. Group 6 was administered LPHNPs. The formulations were delivered every other day through intraperitoneal injection using a 1 cc syringe. Animals were monitored for 1 to 14 days for changes in body weight, mortality, and behavioral patterns. Following 14 days of observation, blood was drawn from mice for hematological and biochemical analysis, and tissues were isolated for histological analysis.

### Relative organ weight calculation

It is an essential metric for assessing toxic impact of nano formulations on the organs of mice following repeated administrations. Organ weight changes were measured after 14 days of treatment. Animals were euthanized through cervical dislocation. Subsequently, the organs were extracted, thoroughly rinsed with saline solution, and weighed. Weight of organs was subsequently compared to those of control group to calculate the organ body weight index using the following formula:

$$\text{Body visceral index (\%)} = \frac{\text{Weight of organ}}{\text{Weight of body}} \times 100$$

----- Equation 6

### Microscopic pathological tissue analysis

To assess potential pathological changes (including abnormalities or lesions) induced by the formulations, histopathological analyses were performed as outlined. In summary, following euthanasia, the major organs were excised and gently rinsed with normal saline. They were then promptly immersed in a 10% formalin solution for preservation. The organs were next encased in paraffin blocks and precisely cut into 0.50 µm thin sections with a rotary microtome. The tissue slices were then adhered to glass slides and

subjected to staining with hematoxylin-eosin and Periodic Acid-Schiff (PAS) reagents. The prepared slides were examined microscopically, and images were captured with a microscope (Ali et al., 2021a).

### Statistical analysis

Graph Pad Prism 9 was used to do one-way ANOVA with post hoc test (Dunnett's multiple comparisons vs control) on remaining data. A significance threshold of  $p < 0.05$  was taken into account when rejecting null hypothesis. Level of significance is expressed as \* $p < 0.05$ , \*\* $p < 0.01$ , \*\*\* $p < 0.001$  and \*\*\*\* $p < 0.0001$

## Results

### Physicochemical profiling

Particle size distribution and surface charges are detailed in Table 1. It is evident that TMX NPs displayed a uniform distribution with a narrow size range of  $194.5 \pm 2.70$  nm and a low polydispersity index of  $0.032 \pm 0.02$ . This was attributed to elevated concentration of emulsifier in nanoparticles, which led to formation of a stable emulsion with smaller and more consistent droplets, thereby producing nanoparticles with reduced size and a low polydispersity index. Incorporating TMX into NPs formulations resulted in a modest increase in particle size, approximately 10–15 nm, and affected size distribution. All nanoparticle formulations displayed a +ve surface charge of  $15.7 \pm 1.60$  mV, which can be attributed to the inclusion of a small quantity of chitosan in formulations. Hydrodynamic diameter was measured at  $100.50 \pm 3.40$  nm with a PDI of  $0.58 \pm 0.06$ , indicating a narrow, monomodal distribution of liposomal vesicles. DOXY LPs exhibited a marginally larger hydrodynamic diameter and PDI. This may be attributed to Doxycycline's tendency to integrate into bilayer membrane, interacting with lipid polar heads via hydrogen bonding, which results in a slight increase in vesicle size. The liposomal formulation exhibited an overall -ve zeta potential  $-14.5 \pm 0.50$  mV. LPHNPs were developed by encasing TMX NPs within DOXY LPs (composed of DPPC/Cholesterol/mPEG2000-DPPE). The hydrodynamic diameter of the LPHNPs was recorded as  $200.4 \pm 2.20$  nm, with no substantial variation in PDI and a zeta potential of  $4.45 \pm 0.50$  mV.

**Table-1:** Physicochemical attributes of TMX-encapsulated PLGA nanoparticles, DOXY-encapsulated liposomes, and lipid-polymer hybrid nanoparticles (LPHNPs) were evaluated. TMX-encapsulated PLGA nanoparticles contains 5 mg of TMX and 100 mg of PLGA. Liposomes comprises 2 mg of DOXY embedded in 10 mg of total lipids. The hydrodynamic diameter is quantified as a function of the intensity-based particle size distribution. Values are expressed as Mean  $\pm$  S.D for 3 independent measurements (n=3).

Formulations	Diameter (nm) $\pm$ SD	PDI $\pm$ SD	$\zeta$ Potential (mV) $\pm$ SD
TMX NP	194.5 $\pm$ 3.20	0.03 $\pm$ 0.02	15.7 $\pm$ 1.51
DOXY LP	100 $\pm$ 2.51	0.25 $\pm$ 0.02	-14.5 $\pm$ 1.32
LPHNPs	200 $\pm$ 2.95	0.07 $\pm$ 0.03	4.45 $\pm$ 1.20

### Efficiency of drug encapsulation (EE%)

Encapsulation efficiencies of TMX NPs and DOXY LPs were measured using solvent extraction. Free drugs were separated from the formulations via centrifugation and ultracentrifugation. A method involving the direct dissolution of nanoparticle or liposomal drug pellet was applied, enabling precise determination of Tamoxifen content in the PLGA nanoparticles and Doxycycline content in the liposomes. The refined nanoparticle formulations displayed a notably high encapsulation efficiency, with Tamoxifen nanoparticles achieving an encapsulation efficiency (EE) of  $85.50 \pm 4.50\%$ . Due to its high hydrophilicity, Doxycycline preferentially positions itself within the hydrophilic environment (polar region) of liposome, resulting in an overall drug loading of  $95.50 \pm 5.10\%$ . The increased encapsulation efficiency (EE) can be attributed to the

solubility of both Tamoxifen and PLGA in ethyl acetate, which is utilized for nanoparticle fabrication. The loading capacities of Tamoxifen nanoparticles and Doxycycline liposomes were measured at  $4.79 \pm 0.52\%$  and  $1.02 \pm 0.41\%$ , respectively.

### Morphological feature analysis

The surface of the nanoparticles suggests a successful encapsulation of Tamoxifen within the PLGA matrix, which is essential for controlled drug release. The uniform size distribution is indicative of a consistent manufacturing process, which is critical for reproducible therapeutic outcomes. The lack of agglomeration observed at higher magnifications implies that the nanoparticles are likely to exhibit stable suspension properties in biological fluids, Figure-1.

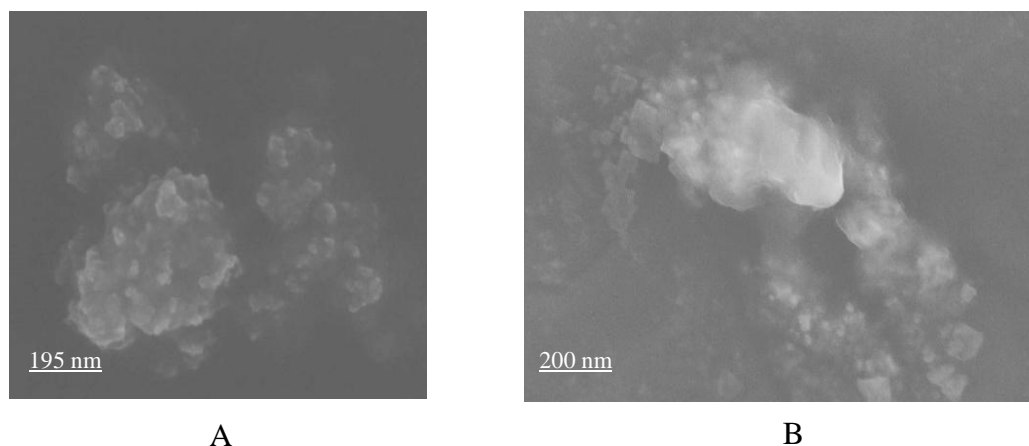


**Figure-1:** (A) SEM image of TMX NPs, (B) SEM image of LPHNPs illustrating the detailed surface morphology.

### ***In vitro* drug dissolution profile**

The *in vitro* release of Tamoxifen from PLGA nanoparticles was conducted in PBS (pH 7.4) with 1% Tween 80, a surfactant that enhances solubility of hydrophobic drugs by forming micelles. Due to Tamoxifen's very low solubility in water, adding a solubility-enhancing component was necessary to maintain sink conditions and achieve detectable UV/VIS conc. during release studies. Grasping drug release mechanisms is vital for managing drug release in polymer formulations designed for sustained delivery applications. Figure-2 shows that Tamoxifen-loaded PLGA nanoparticles display a biphasic release pattern, with a 40% burst release of Tamoxifen within the first 24 hours. The initial burst of drug release was followed by a sustained release over 7 days. Early release primarily resulted from the drug desorbing or diffusing from the nanoparticle surface or loosely bound polymer matrix. Unreleased drug is presumed to be tightly bound to the PLGA molecules or well-trapped within the nanoparticle matrix, with its release primarily driven by diffusion or matrix degradation under sink conditions. When diffusion outpaces matrix erosion, the release mechanism is predominantly controlled by diffusion. Tamoxifen nanoparticles demonstrated a higher cumulative release of 72% (Figure-2), likely due to their smaller size, which provides a larger surface area and thus a greater number of drug molecules available for faster release.

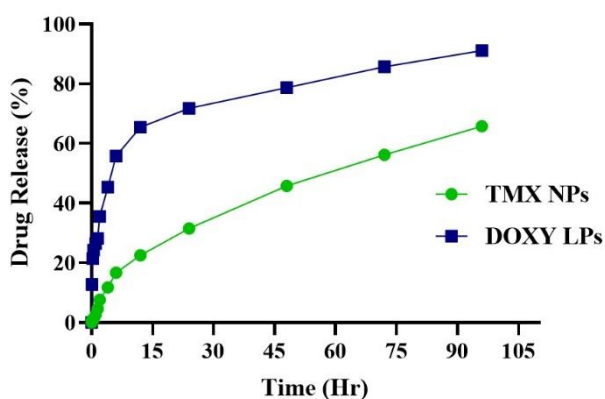


**Figure-2:** Cumulative release (%) of TMX NPs and DOXY LPs was measured in PBS (pH 7.4) containing 1% Tween 80 to ensure sink conditions. Samples taken at specified intervals, evaluated spectrophotometrically.

### ***In vitro* cytotoxicity**

Yellow tetrazolium salt is used in MTT assay. This salt has the ability to lower cellular activity by metabolizing into formazan crystals. They can be computed via spectrophotometric analysis and display UV absorption. The computed absorbance indicates amount of formazan produced by living cells is closely correlated with numerical value of viable cells. *In vitro* cellular toxicity can be illustrated as concentration of nanoformulation increases, % inhibition increases and LPHNPs showed highest % inhibition as compared to free drugs because lipids covered outer surface of PLGA nanoparticles that is favorable for cells and improve cell viability at dose dependency. Highest conc. of LPHNPs showed EPR effect (enhanced permeation effect and retention) at higher dose. These values demonstrate selective toxicity of Lipid coated nanoparticles, which are more effective against cancer cells (MCF-7) while being less toxic to noncancerous cells (Vero). Results of % age cell viability can be seen in the following Figure-3.

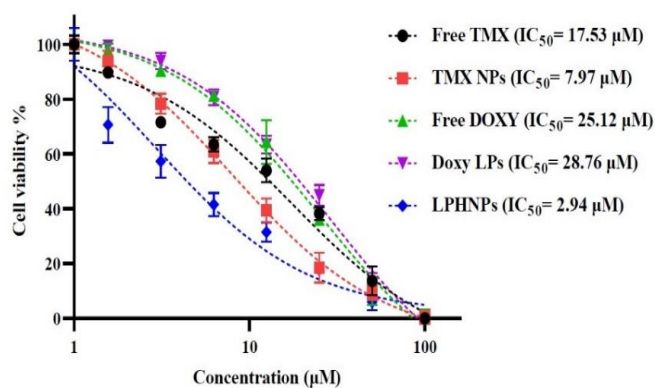


**Figure-3:** Percentage cell viability of MCF-7 cells following treatment with Free TMX, TMX NPs, Free Doxy, Doxy LPs and LPHNPs. Data represent the mean  $\pm$  standard deviation of three independent experiments.

Results indicated that LPHNPs exhibited the highest cytotoxicity on MCF-7 cells as compared to free TMX. While, LPHNPs showed less cytotoxic effect on Vero cells even on high doses as compare to free TMX. Previous literature also showed that nanoformulations of TMX show lowest cell viability than free TMX. Values of selectivity index were calculated using equation. Values of SI for free TMX, TMX NPs, Free DOXY, DOXY LPs and LPHNPs were 2.39, 3.44, 1.11, 5.0 and 48.9 respectively. Values indicated that LPHNPs have synergistic effect as compare to free form, thus achieved targeted delivery of drugs to MCF-7 breast cancer cells with more safe effect on other non-cancerous cells.

### ***In vivo* acute toxicity assessment**

Safety and tolerability of the nanoformulations were assessed in mice by monitoring weight variations, performing serum biochemical tests, and conducting histopathological examinations to evaluate *in vivo* toxicity (Wang et al., 2023). Formulations were administered intraperitoneally to albino mice at doses

of 5 mg/kg for TMX and 80 µg/kg for DOXY. Over 48 hours, no signs of toxicity were observed in behavioral patterns, skin, urine color, respiration, or sleep. There were no deaths or significant weight changes, indicating formulations' safety. After 14 days, blood samples were collected, and mice were euthanized for organ histological analysis (Sani et al., 2023).

### **Relative organ weight**

It serves as a reliable indicator of chemically induced alterations in organs. Assessing comparison of organ weights among untreated and treated animal groups can aid in evaluating toxicity profile of drug formulations (Faria et al., 2021; Haggag et al., 2020). Upon completing a 14-day treatment period, the ratios of organ weight to body weight (visceral indices) for essential organs such as brain, mammary glands, heart, liver, kidneys, lungs, and uterus were computed and are detailed in Table 2. Subsequent to euthanizing animals, organs were meticulously excised and rinsed with normal saline prior to weighing.

**Table-2:** Visceral body index of the subjects after autopsy. Results displayed no significant changes in weight of any organ across all treatments, suggesting formulations' non-toxicity and biocompatibility. Values expressed as mean ± SD, n=6

Parameters (gm)	NC	Free TMX	TMX NPs	Free DOXY	DOXY LPs	LPHNPs
Average Body weight	33.48 ±3.14	30.96 ±3.57	31.26 ±2.37	33.42 ±2.69	32.13 ±3.61	32.98 ±3.18
Brain	0.44±0.01	0.39±0.02	0.40±0.02	0.42±0.01	0.40±0.04	0.43±0.02
Heart	0.17± 0.02	0.15± 0.01	0.15± 0.02	0.15± 0.03	0.16± 0.03	0.16± 0.02
Lungs	0.14±0.14	0.10±0.19	0.11±0.15	0.11±0.11	0.13±0.18	0.14±0.20
Liver	1.47±0.20	1.39±0.28	1.35±0.19	1.41±0.22	1.40±0.21	1.42±0.18
Left Kidney	0.20±0.02	0.17±0.04	0.15±0.02	0.19±0.03	0.22±0.02	0.21±0.04
Right Kidney	0.19±0.02	0.15±0.03	0.13±0.02	0.17±0.02	0.18±0.04	0.19±0.03

### Biochemical screening

Biochemical markers serve as sensitive indicators to assess clinical effects caused by biological treatments, such as nanoformulations. LFTs and RFTs are pivotal in gauging proper functioning of liver and kidneys, respectively. Findings from biochemical analysis of mice blood following treatment with formulations are depicted in Figure 4. Results illustrated, bilirubin levels remained largely unchanged, except for free tamoxifen and free doxycycline. In these treatments, bilirubin levels were slightly elevated compared to control group but remained within acceptable limits. Aminotransferases serve as primary indicator of liver damage. If there is any cellular injury to hepatocytes or bile ducts, alanine transaminase (ALT), gamma glutamyl transferase (GGT), and alkaline phosphatase (ALP) may seep into the bloodstream, leading to elevated systemic levels of these enzymes. The levels of ALP were notably elevated in mice treated with free TMX and DOXY (dissolved in DMSO), as well as in those treated with TMX NP and DOXY LPs, compared to lipid-coated nanoparticles. Additionally,

ALT levels were significantly increased in groups treated with free TMX and DOXY LPs. The elevated levels of both enzymes may suggest liver's effort to detoxify foreign particles and potential inflammation. Moreover, GGT levels were significantly heightened in all treatment groups, with most pronounced increase seen in groups treated with free TMX, TMX NPs, and free DOXY, while no significant effect was observed in group treated with LPHNPs. This could potentially indicate non-alcoholic fatty liver and cardiac issues. Results from renal function tests (RFTs) revealed a moderate increase in creatinine levels with free TMX and TMX NPs compared to control group as shown in Figure 4. However, in all other treatment groups, alterations in these biomarker levels remained statistically insignificant. Blood urea level showed an increase with free DOXY compared to control. This modest increase in biomarker levels may suggest renal hypertrophy and compromised kidney function. No significant changes in creatinine levels were observed in the other treatment groups. These findings from biochemical analysis were consistent with results obtained from body visceral indices.

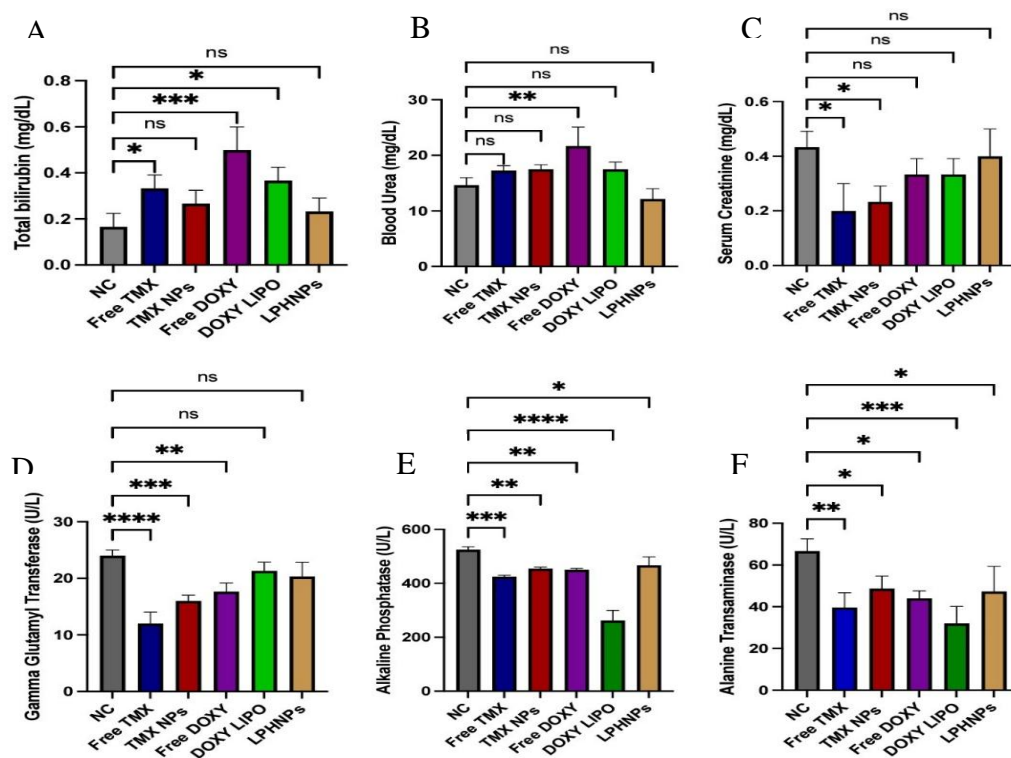


**Figure-4:** Blood biochemical profile consisting of liver function tests (LFTs); (A) Creatinine, (B) Bilirubin, (C) Blood Urea, (D) ALP, (E) AST, (F) GGT values following treatment with nanoformulations are shown as mean  $\pm$  S.D (n=3). Statistical significance is denoted as \*\*\* $p$  < 0.001, \*\* $p$  < 0.01 and \* $p$  < 0.1.

### Hematological analysis

When any exogenous substance, such as pharmaceutical formulations, interacts with blood constituents, it can trigger an immediate inflammatory reaction, potentially leading to complications in the administration of medication. This underscores the need for comprehensive investigation into the potential toxicity of drug formulations and their delivery systems on composition and function of blood. The influence of formed nanoformulations on blood and its components in mice was examined using a complete blood count (CBC) (Rossi et al., 2023). The findings from the hematological analysis are provided in the table below. The outcomes indicated that Platelets and White Blood Cells (WBCs) were significantly influenced during the administration of free Tamoxifen and free Doxycycline, potentially

resulting in thrombocytopenia and leukopenia, respectively. This could potentially stem from bone marrow suppression. These findings underscore the importance of encapsulating free Tamoxifen/Doxycycline within carrier systems that are comparatively less toxic. Tamoxifen nanoparticles (NPs), Doxycycline liposomes, and LPHNPs did not exhibit a notable impact on Hemoglobin and Red Blood Cell (RBC) count. Additionally, other parameters such as mean corpuscular volume (MCV), hematocrit (HCT), mean corpuscular hemoglobin (MCH), and mean corpuscular hemoglobin concentration (MCHC) were monitored. It was observed that these parameters remained relatively stable across all nanoformulations, indicating safety profile of these formulations as shown in Table 3.

**Table-3:** Values of blood biomarkers after Intra peritoneal administration of normal saline, free TMX, TMX nanoparticles, free DOXY, DOXY loaded liposomes and LPHNPS. After 14 days of treatment, blood was withdrawn to test. The values are expressed as mean  $\pm$  S. D (n = 3).

Blood biomarkers	NC	Free TMX	TMX NPs	Free DOXY	DOXY LPs	LPHNPs
WBC ( $\times 10^9/\mu\text{L}$ )	4.8 $\pm$ 0.62	4.5 $\pm$ 0.73	5.6 $\pm$ 0.91	4.4 $\pm$ 0.69	4.1 $\pm$ 0.97	5.7 $\pm$ 0.92
RBC ( $\times 10^6/\mu\text{L}$ )	8.96 $\pm$ 2.21	9.35 $\pm$ 1.72	9.11 $\pm$ 1.98	9.02 $\pm$ 2.43	9.78 $\pm$ 2.13	8.2 $\pm$ 1.79
HGB (gm/dL)	14.4 $\pm$ 2.30	15 $\pm$ 1.95	14.9 $\pm$ 2.36	14.5 $\pm$ 2.19	15.2 $\pm$ 1.16	13.2 $\pm$ 2.25
HCT (%)	43.7 $\pm$ 2.43	54.4 $\pm$ 1.25	50.7 $\pm$ 1.92	51 $\pm$ 2.03	52.8 $\pm$ 1.99	44.2 $\pm$ 2.01
MCV (fL)	43.8 $\pm$ 1.97	58.2 $\pm$ 2.08	55.7 $\pm$ 1.32	56.5 $\pm$ 2.03	54 $\pm$ 0.22	53.9 $\pm$ 0.83
MCH (pg)	16.1 $\pm$ 0.77	16.8 $\pm$ 0.91	16.4 $\pm$ 0.89	16.1 $\pm$ 0.79	15.5 $\pm$ 0.82	16.2 $\pm$ 0.87
MCHC (g/dL)	33.1 $\pm$ 0.26	27.6 $\pm$ 0.21	29.4 $\pm$ 0.31	28.4 $\pm$ 0.19	28.8 $\pm$ 0.26	29.9 $\pm$ 0.34
PLT ( $\times 10^3/\mu\text{L}$ )	769 $\pm$ 31	592 $\pm$ 23	788 $\pm$ 30	518 $\pm$ 38	693 $\pm$ 29	736 $\pm$ 19
LYM (%)	83.1 $\pm$ 1.20	90.2 $\pm$ 1.31	91.2 $\pm$ 1.81	85.4 $\pm$ 1.35	90 $\pm$ 2.01	87.4 $\pm$ 1.12
RDW-SD (fL)	20.7 $\pm$ 2.13	49.5 $\pm$ 1.39	48.9 $\pm$ 1.41	45.6 $\pm$ 0.92	44.2 $\pm$ 0.53	30.1 $\pm$ 1.22
RDW-CV %	24.5 $\pm$ 0.25	24.3 $\pm$ 0.51	25.6 $\pm$ 0.72	22.9 $\pm$ 0.18	25.2 $\pm$ 0.70	25.9 $\pm$ 0.64
PDW (%)	9.9 $\pm$ 0.20	9.5 $\pm$ 0.49	10.3 $\pm$ 0.78	9.6 $\pm$ 0.92	8.7 $\pm$ 0.97	9.1 $\pm$ 1.20
MPV (fL)	10.2 $\pm$ 0.43	8.7 $\pm$ 0.31	7.9 $\pm$ 0.49	7.5 $\pm$ 1.27	6.9 $\pm$ 1.07	7.6 $\pm$ 2.81
P-LCR (%)	14.8 $\pm$ 0.61	10.7 $\pm$ 0.83	12.1 $\pm$ 0.29	10.2 $\pm$ 0.39	6.1 $\pm$ 1.01	9.8 $\pm$ 1.32

### Histopathological examinations

A significant challenge in the clinical application of anticancer agents is the risk of peripheral tissue damage, potentially resulting in multi-organ toxicity (Chakraborti et al., 2022). To evaluate potential toxicity in the organs of mice treated with the formulations, both biochemical and histological analyses were conducted. Sections of key organs brain, breast, heart, kidney, and liver were prepared using a rotary microtome. Tissue slices were mounted on glass slides, stained with H&E, and examined microscopically. Hematoxylin stained the cell nuclei blue, while eosin stained the cytoplasm and extracellular matrix pink. Healthy cells were identified by their polygonal shape and blue nuclei, which were either spherical or spindle shaped. In contrast, necrotic cells displayed pink amorphous material in the cytoplasm with absent nuclei. Apoptotic cells appeared shrunken and rounded, with condensed and darkened nuclei (Chan, 2014). The tissue section images are depicted in Figure 5. It can be observed that degeneration or pyknosis and absence of axons in brain showed in TMX loaded PLGA NPs, while remaining treatment groups did not show any

abnormality (Han et al., 2020). Breast samples were showed mild chronic inflammation and intraductal secretions in the group that was treated with tamoxifen loaded PLGA nanoparticles, and remaining groups showed no sign of necrosis, hemorrhage or chronic inflammation (Passos et al., 2023). Tissues of heart samples from all treatment groups exhibited no abnormalities and appeared entirely normal. There were no noticeable signs of necrosis and edema, but slight muscular thickness and muscular distortion can be seen. Kidney has not showed signs of necrosis and apoptosis, but congestion of renal tissue due to acute inflammation can be seen in treatment groups (E Owumi et al., 2021). Liver sections from all treatment groups appeared normal, with no alterations in fat tissue, except for group treated with free TMX. It exhibited signs of focal lobular necrosis, inflammation, and apoptosis of hepatic cells (Koller et al., 2021). No indications of necrotic cells or hydrophobic degradation were detected in any treatment groups. These results affirm the safety of our lipid-coated particles, as all histological analyses showed no evidence of toxicity.

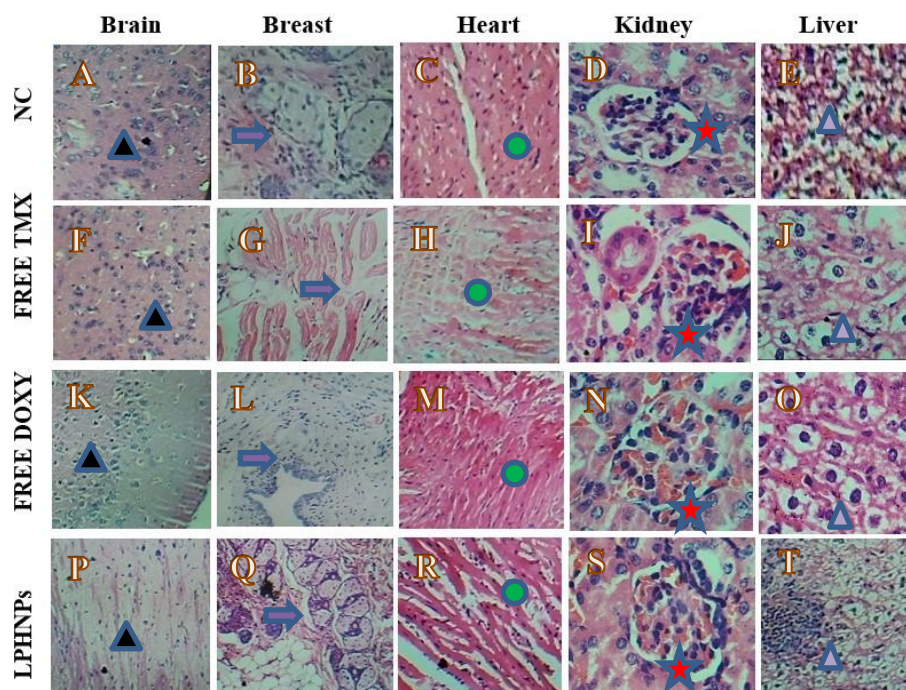


**Figure-5:** Histological examination of different organs was conducted following treatment with free TMX, free DOXY and LPHNPs. Animals treated with NS 0.9 % served as negative control (NC). A, F, K, P images: brain tissues, B, G, L, Q: breast tissues, C, M, H, R: heart tissues, D, I, N, S: kidney tissues and E, J, O, T: liver tissues. Hematoxylin and eosin dyes used on tissues to evaluate impact of treatments on organ structure and cellular integrity. Black triangle: brain cells, Yellow arrows: breast cells, green circles: cardiac cells, Red star: bowman's capsule with normal glomeruli and Yellow triangle: normal hepatocytes with round nucleus.

## Discussion

Tamoxifen is extensively utilized in breast cancer treatment; however, similar to many cancer therapies, it also poses side effects by causing significant damage to normal cells. Specifically, tamoxifen is known to increase the risk of endometrial and liver cancers, that restricts its therapeutic application for longer period of time (Jena and Sangamwar, 2017; Kassem et al., 2018). The primary undesirable effects of tamoxifen are dependent on dosage and conc. By maintaining consistent dosing over time or by combining TMX with other cytotoxic drugs these effects can be mitigated. Nanomedicine offers several advantages over conventional cancer therapies. These include reduced breakdown of drug during transport, shielded from *in vivo* chemical or biological conditions, reduced undesirable effects through improved biocompatibility, enhanced targeting and increased delivery of chemotherapy specifically to cancerous tissues. Nanomedicine holds significant potential for selectively targeting and eliminating breast cancer stem cells, crucial for initiating, recurring, and developing resistance to chemotherapy and radiotherapy in breast cancer treatment (Afzal et al., 2021; Hejmady et al., 2020). Nanotechnology has significantly advanced the delivery of therapeutic drugs directly to cancerous tissues, minimizing harm to healthy tissues. This approach enhances drug elimination from body, improves bioavailability, facilitates precise delivery of conjugated drugs to such tissues that are cancerous, enhances efficacy, allows for sustained release, and supports dose maintenance. Several nano delivery systems have been utilized to transport tamoxifen molecules, enabling selective delivery to cancerous tissues of breast with high precision and minimal side effects to surrounding healthy cells. This approach harnesses the drug's beneficial properties while reducing cytotoxicity associated with non-targeted delivery (Bhagwat et al., 2020; Day et al., 2018; Jena and Sangamwar, 2017). TMX-loaded NPs were formulated using solvent evaporation method, DOXY-loaded NPs were formulated via film hydration method, and lipid-polymer hybrid nanoparticles were synthesized using the fusion method in this study (Maji et al., 2014; Mohanty et al., 2020; Pandey et al., 2015; Umbarkar et al., 2021; Yu et al., 2020). Combining tamoxifen with fatostatin has been shown to synergistically inhibit ER-positive breast cancer, enhancing both safety and efficacy (Liu et al., 2020). Doxycycline has been demonstrated to synergize with doxorubicin in

combating division of castration-resistant prostate cancer cells (Zhu et al., 2017). In another study, combination of doxycycline with azithromycin and vitamin C (DAV) proved to be a potent therapy for targeting mitochondria and eliminating cancer stem cells (CSCs) (Fiorillo et al., 2019). These combinations have been shown to be safe in previous studies and have improved efficacy of nanocarriers in delivering drugs to cancer tissues (Chauhan and Srivastava, 2015; Jain et al., 2011). The central focus of this study was the formation of a novel nanocarrier system capable of delivering two distinct therapeutic agents to cancer cells. This nanocarrier represents an advancement over conventional drug delivery systems by incorporating two different drugs within a single carrier to effectively treat breast cancer. These nanoparticles allow for encapsulation of both hydrophobic and hydrophilic drugs in distinct compartments: tamoxifen in core, and doxycycline in lipid bilayer shell. This system enhances therapeutic efficacy, circulation time, and drug bioavailability and reducing side effects in peripheral tissues (Massadeh et al., 2020; Penheiro, 2017). Formed nanoformulations underwent comprehensive evaluation for their physicochemical characteristics, *in vitro* and *in vivo* performance, and biocompatibility. Following preliminary assessments, the top-performing liposomes, were combined to create a unified liposome structure, which was then applied as a coating over the tamoxifen nanoparticles (Mohanty et al., 2020). The developed lipoparticles underwent physicochemical characterization, with particle size being a crucial parameter. Nano carriers smaller than 1  $\mu\text{m}$  can easily traverse vasculature, facilitating enhanced penetration in malignant tissues due to increased vascularity. Nano sized particles can efficiently traverse membranes and exhibit distinct accumulation patterns in tumor tissues and more effectively internalized by cells through endocytosis compared to larger particles (Dolai et al., 2021). The particle sizes of TMX NPs, DOXY LPs, and LPHNPs were determined to be  $198 \pm 3.2$  nm,  $100.5 \pm 4.2$  nm, and  $200 \pm 2.5$  nm, respectively. The lipoparticles showed a slight increase in size by approximately 4-5 nm compared to the uncoated nanoparticles, which was consistent with findings from surface morphological studies. The entrapment efficiencies (EE%) of Tamoxifen-loaded PLGA nanoparticles and Doxycycline-loaded liposomes were found to be  $95.31\% \pm 0.76\%$  and  $92.32\% \pm 1.5\%$ , respectively. These values are consistent with a previously reported

result (85.7%) for polymer-lipid nanoparticles in prior research (Jeong et al., 2001). It could be inferred that lipid-polymer hybrid nanoparticles (LPHNPs) may offer improved drug entrapment. Drug loading was seen to increase in direct relation to the amount of drug added during the formulation process, up to a certain approximate limit. *In vitro* drug release showed a dual pattern with an initial burst release followed by sustained release over subsequent days. Additionally, higher therapeutic efficacy of lipoparticles was demonstrated through *in vitro* cytotoxicity synergism. After treating MCF-7 cells with nanoparticles, the viability of cells decreased as the concentration of particles increased, as measured 24 hours post-incubation with various conc. of NPs, LPs, and LPHNPs (Lazzeroni et al., 2012).

### Conclusion and future suggestion

Based on these results, it can be inferred that the creation of this innovative nanocarrier system shows potential for concurrently delivering multiple medications to breast cancer cells with minimal toxicity. The findings support further development of surface modified nano formulations and clinical testing of the formulation as a potential preventive treatment for breast cancer. The next steps should involve detailed mechanistic studies and long-term efficacy assessments to fully understand the formulation's protective mechanisms and its potential for clinical application.

### Acknowledgments

We would like to express our sincere gratitude to all those who contributed to the completion of this research. We would also like to acknowledge the support of WTO laboratory, which provided the necessary resources and facilities for this research.

**Disclaimer:** None

**Conflict of Interest:** None

**Source of Funding:** None

### Contribution of Authors

Qurat ul Ain: Writing original draft preparation, methodology, experiment performance & software.

Rasheed MA: Conceptualization, supervision, reviewing & editing.

Tariq I: Conceptualization, methodology, visualization & investigation.

Omar MO: Supervision & reviewing.

Zahoor MY: Software, methodology, reviewing & editing.

### References

- Abdmouleh F, El Arbi M, Saad HB, Jellali K, Ketata E, Amara IB, Pigeon P, Hassen HB, Top S and Jaouen G, 2020. Antimicrobial, antitumor and side effects assessment of a newly synthesized tamoxifen analog. *Curr Top Med Chem.* 20(25): 2281-2288. DOI: 10.2174/1568026620666200819145526
- Afzal M, Alharbi KS, Alruwaili NK, Al-Abassi FA, Al-Malki AAL, Kazmi I, Kumar V, Kamal MA, Nadeem MS and Aslam M, 2021. *Semin Cancer Biol.* DOI: 10.1016/j.semcancer.2019.12.016
- Ahmad R, Kaus NHM and Hamid S, 2020. Synthesis and characterization of PLGA-PEG thymoquinone nanoparticles and its cytotoxicity effects in tamoxifen-resistant breast cancer cells. *Adv Exp Med Biol.* DOI: 10.1007/5584\_2018\_302
- Ali A, Saeed S, Hussain R, Afzal G, Siddique AB, Parveen G, Hasan M and Caprioli G, 2023. Synthesis and characterization of silica, silver-silica, and zinc oxide-silica nanoparticles for evaluation of blood biochemistry, oxidative stress, and hepatotoxicity in albino rats. *ACS omega.* 8(23): 20900-20911. DOI: 10.1021/acsomega.3c01674
- Ali S, Amin MU, Tariq I, Sohail MF, Ali MY, Preis E, Ambreen G, Pinnapireddy SR, Jedelská J and Schäfer J, 2021a. Lipoparticles for synergistic chemo-photodynamic therapy to ovarian carcinoma cells: in vitro and in vivo assessments. *Int J Nanomedicine.* 951-976. DOI: 10.2147/IJN.S285950
- AlMajed Z, Salkho NM, Sulieman H and Hussein GA, 2022. Modeling of the in vitro release kinetics of sonosensitive targeted liposomes. *Biomédicines.* 10(12): 3139. DOI: 10.3390/biomedicines10123139
- Bhagwat GS, Athawale RB, Gude RP, Md S, Alhakamy NA, Fahmy UA and Kesharwani P, 2020. Formulation and development of transferrin targeted solid lipid nanoparticles for breast cancer therapy. *Front Pharmacol.*

- 11: 614290.  
DOI: 10.3389/fphar.2020.614290
- Chakraborti S, Stewart A and Maity B, 2022. Impact of Chemotherapeutic Drugs Towards Oxidative Stress and Associated Multi-organ Physiological Responses. In: Handbook of Oxidative Stress in Cancer: Therapeutic Aspects. Springer. p. 3961-3985.
- Chan JK, 2014. The wonderful colors of the hematoxylin–eosin stain in diagnostic surgical pathology. *Int J Surg Pathol.* 22(1): 12-32. DOI: 10.1177/1066896913517939
- Chhipa RR, Singh S, Surve SV, Vijayakumar MV and Bhat MK, 2005. Doxycycline potentiates antitumor effect of cyclophosphamide in mice. *Toxicol Appl Pharmacol.* 202(3): 268-277. DOI: 10.1016/j.taap.2004.06.025
- Day CM, Parikh A, Song Y and Garg S, 2018. Nanotechnology and Nature's Miracle Compound: Curcumin. In: *NanoNutraceuticals*. CRC Press. p. 213-254.
- Dolai J, Mandal K and Jana NR, 2021. Nanoparticle size effects in biomedical applications. *ACS Appl Nano Mater.* 4(7): 6471-6496. DOI: <https://doi.org/10.1021/acsanm.1c00987>
- Duse L, Agel MR, Pinnapireddy SR, Schäfer J, Selo MA, Ehrhardt C and Bakowsky U, 2019. Photodynamic therapy of ovarian carcinoma cells with curcumin-loaded biodegradable polymeric nanoparticles. *Pharmaceutics.* 11(6): 282. DOI:10.3390/pharmaceutics11060282
- E Owumi S, K Olusola J, O Arunsi U and K Oyelere A, 2021. Chlorogenic acid abates oxido-inflammatory and apoptotic responses in the liver and kidney of Tamoxifen-treated rats. *Toxicol Res.* 10(2): 345-353. DOI: 10.1093/toxres/tfab002
- Faria RS, de Lima LI, Bonadio RS, Longo JPF, Roque MC, de Matos Neto JN, Moya SE, de Oliveira MC and Azevedo RB, 2021. Liposomal paclitaxel induces apoptosis, cell death, inhibition of migration capacity and antitumoral activity in ovarian cancer. *Biomed Pharmacother.* 142: 112000. DOI: 10.1016/j.biopha.2021.112000
- Fife RS and Sledge Jr GW, 1995. Effects of doxycycline on in vitro growth, migration, and gelatinase activity of breast carcinoma cells. *J Lab Clin Med.* 125(3): 407-411.
- Fiorillo M, Tóth F, Sotgia F and Lisanti MP, 2019. Doxycycline, Azithromycin and Vitamin C (DAV): A potent combination therapy for targeting mitochondria and eradicating cancer stem cells (CSCs). *Aging (Albany NY).* 11(8): 2202.
- Gu Y, Lee M, Roemer J, Musacchia L, Golub M and Simon R, 2001. Inhibition of tumor cell invasiveness by chemically modified tetracyclines. *Curr Med Chem.* 8(3): 261-270. DOI: 10.2174/0929867013373642
- Haggag YA, Ibrahim RR and Hafiz AA, 2020. Design, formulation and in vivo evaluation of novel honokiol-loaded PEGylated PLGA nanocapsules for treatment of breast cancer. *Int J Nanomedicine.* 1625-1642. DOI: 10.2147/IJN.S241428
- Han S, Nandy P, Austria Q, Siedlak SL, Torres S, Fujioka H, Wang W and Zhu X, 2020. Mfn2 ablation in the adult mouse hippocampus and cortex causes neuronal death. *Cells.* 9(1): 116. DOI: 10.3390/cells9010116
- Hejmady S, Pradhan R, Alexander A, Agrawal M, Singhvi G, Gorain B, Tiwari S, Kesharwani P and Dubey SK, 2020. Recent advances in targeted nanomedicine as promising antitumor therapeutics. *Drug Discov Today.* 25(12): 2227-2244. DOI: 10.1016/j.drudis.2020.09.031
- Ismail A, Mokhlis HA, Sharaky M, Sobhy MH, Hassanein SS, Doghish AS, Salama SA, Mariee AD, Attia YMJP-R and Practice, 2022. Hydroxycitric acid reverses tamoxifen resistance through inhibition of ATP citrate lyase. 240: 154211. DOI: 10.1016/j.prp.2022.154211
- Jain AK, Swarnakar NK, Godugu C, Singh RP and Jain S, 2011. The effect of the oral administration of polymeric nanoparticles on the efficacy and toxicity of tamoxifen. *Biomaterials.* 32(2): 503-515. DOI: 10.1016/j.biomaterials.2010.09.037
- Jena SK and Sangamwar AT, 2017. Polymeric micelles: a promising tool for tamoxifen delivery in cancer? In: Taylor & Francis. p. 109-111. DOI: <https://doi.org/10.4155/tde-2016-0083>
- Jeong YI, Cho CS, Kim SH, Ko KS, Kim SI, Shim YH and Nah JW, 2001. Preparation of poly (DL-lactide-co-glycolide) nanoparticles

- without surfactant. *J Appl Polym Sci.* 80(12): 2228-2236. DOI:10.1002/APP.1326
- Karami LJS, 2023. Interaction of neutral and protonated Tamoxifen with the DPPC lipid bilayer using molecular dynamics simulation. *194:* 109225. DOI:10.1016/j.steroids.2023.109225
- Kassem MA, Megahed MA, Abu Elyazid SK, Abd-Allah FI, Abdelghany TM, Al-Abd AM and El-Say KM, 2018. Enhancing the therapeutic efficacy of tamoxifen citrate loaded span-based nano-vesicles on human breast adenocarcinoma cells. *AAPS PharmSciTech.* 19: 1529-1543. DOI: 10.1208/s12249-018-0962-y
- Koller T, Vrbova P, Meciarova I, Molcan P, Smitka M, Selcanova SA and Skladany L, 2021. Liver injury associated with the use of selective androgen receptor modulators and post-cycle therapy: Two case reports and literature review. *World J Clin Cases.* 9(16): 4062. DOI: 10.12998/wjcc.v9.i16.4062
- Lafi Z, Alshaer W, Ma'mon MH, Zihlif M, Alqudah DA, Nsairat H, Azzam H, Aburjai T, Bustanji Y and Awidi A, 2021. Aptamer-functionalized pH-sensitive liposomes for a selective delivery of echinomycin into cancer cells. *RSC advances.* 11(47): 29164-29177. DOI: <https://doi.org/10.1039/D1RA05138E>
- Lazzeroni M, Serrano D, Dunn BK, Heckman-Stoddard BM, Lee O, Khan S and Decensi A, 2012. Oral low dose and topical tamoxifen for breast cancer prevention: modern approaches for an old drug. *Breast Cancer Res.* 14: 1-11. DOI: 10.1186/bcr3233
- Lin M and Qi X-R, 2021. Purification method of drug-loaded liposome. *Liposome-based drug delivery systems.* 111-121. DOI: [https://doi.org/10.1007/978-3-662-49320-5\\_24](https://doi.org/10.1007/978-3-662-49320-5_24)
- Liu Y, Jiang M, Tu Y, Wang K, Zong Q and Yuan YJB, 2021. Time-programmed activation of dual polyprodrugs for synergistic cascade oxidation-chemotherapy. *278:* 121136. DOI: 10.1016/j.biomaterials.2021.121136
- Liu Y, Zhang N, Zhang H, Wang L, Duan Y, Wang X, Chen T, Liang Y, Li Y and Song X, 2020. Fatostatin in combination with tamoxifen induces synergistic inhibition in ER-positive breast cancer. *Drug Des Dev Ther.* 3535-3545. DOI: 10.2147/DDDT.S253876
- Mahmoud G, Jedelská J, Omar SM, Strehlow B, Schneider M and Bakowsky U, 2018. Stabilized tetraether lipids based particles guided porphyrins photodynamic therapy. *Drug Deliv.* 25(1): 1526-1536. DOI: 10.1080/10717544.2018.1482970
- Maji R, Dey NS, Satapathy BS, Mukherjee B and Mondal S, 2014. Preparation and characterization of Tamoxifen citrate loaded nanoparticles for breast cancer therapy. *Int J Nanomedicine.* 3107-3118. DOI: 10.2147/IJN.S63535
- Markowska A, Kaysiewicz J, Markowska J and Huczyński A, 2019. Doxycycline, salinomycin, monensin and ivermectin repositioned as cancer drugs. *Bioorg Med Chem Lett.* 29(13): 1549-1554. DOI: 10.1016/j.bmcl.2019.04.045
- Massadeh S, Omer ME, Alterawi A, Ali R, Alanazi FH, Almutairi F, Almotairi W, Alobaidi FF, Alhelal K and Almutairi MS, 2020. Optimized polyethylene glycolylated polymer-lipid hybrid nanoparticles as a potential breast cancer treatment. *Pharmaceutics.* 12(7): 666. DOI: 10.3390/pharmaceutics12070666
- Mohanty A, Uthaman S and Park I-K, 2020. Utilization of polymer-lipid hybrid nanoparticles for targeted anti-cancer therapy. *Molecules.* 25(19): 4377. DOI: 10.3390/molecules25194377
- Moin A, Wani SUD, Osmani RA, Abu Lila AS, Khafagy E-S, Arab HH, Gangadharappa HV and Allam AN, 2021. Formulation, characterization, and cellular toxicity assessment of tamoxifen-loaded silk fibroin nanoparticles in breast cancer. *Drug Deliv.* 28(1): 1626-1636. DOI: 10.1080/10717544.2021.1958106
- Nankali E, Shaabanzadeh M and Torbati MB, 2020. Fluorescent tamoxifen-encapsulated nanocapsules functionalized with folic acid for enhanced drug delivery toward breast cancer cell line MCF-7 and cancer cell imaging. *Naunyn Schmiedebergs Arch*

- Pharmacol. 393(7): 1211-1219.  
DOI: 10.1007/s00210-020-01825-1
- Onoda T, Ono T, Dhar DK, Yamanoi A, Fujii T and Nagasue N, 2004. Doxycycline inhibits cell proliferation and invasive potential: combination therapy with cyclooxygenase-2 inhibitor in human colorectal cancer cells. *J Lab Clin Med.* 143(4): 207-216.  
DOI: 10.1016/j.lab.2003.12.012
- Onoda T, Ono T, Dhar DK, Yamanoi A and Nagasue N, 2006. Tetracycline analogues (doxycycline and COL-3) induce caspase-dependent and-independent apoptosis in human colon cancer cells. *Int J Cancer.* 118(5): 1309-1315.  
DOI: 10.1002/ijc.21447
- Pandey SK, Ghosh S, Maiti P and Haldar C, 2015. Therapeutic efficacy and toxicity of tamoxifen loaded PLA nanoparticles for breast cancer. *Int. J. Biol. Macromol.* 72: 309-319.  
DOI: 10.1016/j.ijbiomac.2014.08.012
- Passos JS, Dartora VF, Salata GC, Malago ID and Lopes LB, 2023. Contributions of nanotechnology to the intraductal drug delivery for local treatment and prevention of breast cancer. *Int J Pharm.* 635: 122681.  
DOI: 10.1016/j.ijpharm.2023.122681
- Pérez E, Benito M, Teijon C, Olmo R, Teijón JM and Blanco MD, 2012. Tamoxifen-loaded nanoparticles based on a novel mixture of biodegradable polyesters: characterization and in vitro evaluation as sustained release systems. *J. Microencapsul.* 29(4): 309-322.  
DOI: 10.3109/02652048.2011.651496
- Rasool M, Rasool MH, Khurshid M and Aslam B, 2024. Biogenic synthesis and characterization of silver nanoparticles: exploring antioxidant and anti-inflammatory activities and assessing antimicrobial potential against multidrug-resistant bacteria. *Asian J. Agric. Biol.* 2024(3): 2023364. DOI: <https://doi.org/10.35495/ajab.2023.364>
- Rossi M, Salomon A, Chaumontel N, Molet J, Bailly S, Tillet E and Bouvard C, 2023. Warning regarding hematological toxicity of tamoxifen activated CreERT2 in young Rosa26CreERT2 mice. *Sci Rep.* 13(1): 5976.  
DOI: 10.1038/s41598-023-32633-1
- Rubins JB, Charboneau D, Alter MD, Bitterman PB and Kratzke RA, 2001. Inhibition of mesothelioma cell growth in vitro by doxycycline. *J Lab Clin Med.* 138(2): 101-106. DOI: 10.1067/mlc.2001.116591
- Saif MS, Waqas M, Hussain R, Ahmed MM, Tariq T, Batool S, Liu Q, Mustafa G and Hasan M, 2024a. Potential of CME@ ZIF-8 MOF Nanoformulation: Smart Delivery of Silymarin for Enhanced Performance and Mechanism in Albino Rats. *ACS Appl Bio Mater.* 7(10): 6919-6931.  
DOI: 10.1021/acsabm.4c01019
- Saif MS, Waqas M, Hussain R, Tariq T, Batool S, Khan I, Ghorbanpour M, Ahmed MM, Sumra AA and Mustafa G, 2024b. Improving the bioavailability of three-dimensional ZIF-8 MOFs against carbon tetrachloride-induced brain and spleen toxicity in rats. *Mater Chem. Phys.* 328: 129997.  
DOI: 10.1016/j.matchemphys.2024.129997
- Sani A, Pourmadadi M, Shaghghi M, Eshaghi MM, Shahmollaghamsary S, Arshad R, Fathikarkan S, Rahdar A, Jadoun S and Medina DI, 2023. Revolutionizing anticancer drug delivery: Exploring the potential of tamoxifen-loaded nanoformulations. *J Drug Deliv Sci Technol.* 104642.  
DOI: 10.1016/j.jddst.2023.104642
- Schäfer J, Sitterberg J, Ehrhardt C, Kumar M and Bakowsky U, 2008. *Adv Sci Technol.* DOI: <https://doi.org/10.1039/c8pp00267c>
- Seftor RE, Seftor EA, De Larco JE, Kleiner DE, Leferson J, Stetler-Stevenson WG, McNamara TF, Golub LM and Hendrix MJ, 1998. Chemically modified tetracyclines inhibit human melanoma cell invasion and metastasis. *Clin. Exp. Metastasis.* 16: 217-225. DOI: 10.1023/a:1006588708131
- Senthilraja P and Kathiresan K, 2015. In vitro cytotoxicity MTT assay in Vero, HepG2 and MCF-7 cell lines study of Marine Yeast. *J. Appl. Pharm. Sci.* 5(3): 080-084.  
DOI: 10.7324/JAPS.2015.50313
- Sharmin M and Bhuiyan A, 2019. Modifications in structure, surface morphology, optical and electrical properties of ZnO thin films with low boron doping. *J. Mater Sci. Mater Electron.* 30(5): 4867-4879.  
DOI: 10.1007/s10854-019-00781-8
- Umbarkar M, Thakare S, Suresh T, Giri A and Chopade V, 2021. Formulation and evaluation of liposome by thin film hydration method. *J.*

- Drug Deliv. Ther. 11(1): 72-76. DOI: <https://doi.org/10.22270/jddt.v11i1.4677>
- Verma P and Maheshwari SK, 2018. Preparation of silver and selenium nanoparticles and its characterization by dynamic light scattering and scanning electron microscopy. *J. Microsc. Ultrastruct.* 6(4): 182. DOI: [10.4103/JMAU.JMAU\\_3\\_18](https://doi.org/10.4103/JMAU.JMAU_3_18)
- Wang W, Xiong Y, Hu X, Lu F, Qin T, Zhang L, Guo E, Yang B, Fu Y and Hu D, 2023. Codelivery of adavosertib and olaparib by tumor-targeting nanoparticles for augmented efficacy and reduced toxicity. *Acta Biomater.* 157: 428-441. DOI: [10.1016/j.actbio.2022.12.021](https://doi.org/10.1016/j.actbio.2022.12.021)
- Yang Z-Z, Zhang Y-Q, Wang Z-Z, Wu K, Lou J-N and Qi X-R, 2013. Enhanced brain distribution and pharmacodynamics of rivastigmine by liposomes following intranasal administration. *Int J Pharm.* 452(1-2): 344-354. DOI: [10.1016/j.ijpharm.2013.05.009](https://doi.org/10.1016/j.ijpharm.2013.05.009)
- Yu X, Sun L, Tan L, Wang M, Ren X, Pi J, Jiang M and Li N, 2020. Preparation and characterization of PLGA-PEG-PLGA nanoparticles containing solidoside and tamoxifen for breast cancer therapy. *AAPS PharmSciTech.* 21: 1-11. DOI: [10.1208/s12249-019-1523-8](https://doi.org/10.1208/s12249-019-1523-8)
- Zeng L, Li W and Chen C-S, 2020. Breast cancer animal models and applications. *Zool Res.* 41(5): 477. DOI: [10.24272/j.issn.2095-8137.2020.095](https://doi.org/10.24272/j.issn.2095-8137.2020.095)
- Zhang X-M, Patel AB, de Graaf RA and Behar KL, 2004. Determination of liposomal encapsulation efficiency using proton NMR spectroscopy. *Chem Phys Lipids.* 127(1): 113-120. DOI: [10.1016/j.chemphyslip.2003.09.013](https://doi.org/10.1016/j.chemphyslip.2003.09.013)
- Zhu C, Yan X, Yu A and Wang Y, 2017. Doxycycline synergizes with doxorubicin to inhibit the proliferation of castration-resistant prostate cancer cells. *Acta Biochim Biophys Sin.* 49(11): 999-1007. DOI: [10.1093/abbs/gmx097](https://doi.org/10.1093/abbs/gmx097)